

HyPlan: Hybrid Learning-Assisted Planning Under Uncertainty for Safe Autonomous Driving

Donald Pfaffmann¹, Matthias Klusch² and Marcel Steinmetz³

Abstract—We present a novel hybrid learning-assisted planning method, named HyPlan, for solving the collision-free navigation problem for self-driving cars in partially observable traffic environments. HyPlan combines methods for multi-agent behavior prediction, deep reinforcement learning with proximal policy optimization and approximated online POMDP planning with heuristic confidence-based vertical pruning to reduce its execution time without compromising safety of driving. Our experimental performance analysis on the CARLA-CTS2 benchmark of critical traffic scenarios with pedestrians revealed that HyPlan may navigate safer than selected relevant baselines and perform significantly faster than considered alternative online POMDP planners.

I. INTRODUCTION

In general, the collision-free navigation (CFN) problem for a self-driving car is to minimize the time to a given goal while avoiding collisions with other objects such as other cars, pedestrians and cyclists in a partially observable traffic environment. This constrained optimization problem can be modeled as a POMDP and solved online by the autonomous vehicle (AV). Major classes of the CFN problem solving methods are based on deep learning [12], [18], [20], [22] including LLMs [6], [8], [13], [30], explicit rule-based [10] and POMDP action planning [4], [25], and hybrid combinations of thereof [3], [9], [10], [17], [27], [28]. While hybrid neuro-explicit planning methods such as LEADER [9], LFGnav [28] and HyLEAP [27] may navigate reasonably safe with provably correct action planning under uncertainty, they still suffer from significantly slower execution times compared to deep learning-based methods. The main reason is their use of explicit but computationally expensive approximate online POMDP planners. One challenge is to close this performance gap in terms of execution time and time to goal without compromising safety of driving.

To address this challenge, we developed HyPlan, a novel hybrid learning-assisted planning method for collision-free navigation of self-driving cars. This hybrid method leverages multi-agent behavior prediction, ego-car path planning, explicit online POMDP planning guided by a PPO-based deep reinforcement learner, and a recent approach for reducing neural network prediction errors, in order to obtain approximately optimal car control action policies quickly. We conducted a comparative experimental analysis on the CARLA-CTS2 benchmark of critical traffic scenes with pedestrian

crossings simulated in CARLA ¹, considering selected state-of-the-art baselines. Among others, the experimental results revealed that HyPlan may navigate safer than all baselines and plan its actions significantly faster than the considered alternative explicit and hybrid POMDP planners. HyPlan is open-source available ².

The remainder of the paper is structured as follows. In Section 2, we describe the considered CFN problem as POMDP and present our novel hybrid solution HyPlan in Section 3, while the experimental evaluation results are summarized in Section 4, before we conclude in Section 5.

II. PROBLEM DESCRIPTION

The problem of finding control actions for a self-driving car to solve the CFN problem in a partially observable traffic environment can be cast as a discrete-time POMDP $(S, A, T, R, \gamma, Z, O)$. The *states* $S = \mathcal{C} \times \dots \times \mathcal{C}$ describe the current traffic situation exactly, assuming one single ego-car and n exogenous agents. The configuration space of each agents is $\mathcal{C} = \mathbb{R}^2 \times \mathbb{R}^2 \times \mathbb{R}^2 \times [0, 2\pi)$, where a state $s_t^x = (p_t^x, p_{\text{goal}}^x, v_t^x, \theta_t^x) \in \mathcal{C}$ of the agent x at time step t specifies the agent's current and goal positions p_t^x and p_{goal}^x , the velocity v_t^x , and the orientation θ_t^x . For the ego-car, the entire state s_t^c is observable, while for the exo-agents e , only p_t^e is observable, if e is not occluded. The *observations* are hence given by $Z = \mathcal{C} \times \mathbb{R}^2 \times \dots \times \mathbb{R}^2$ with *observation probabilities* $O(s_t, a_t, o_t) = T(s_{t+1}|s_t, a_t)$ for $o = (s_{t+1}^c, p_{t+1}^{e_1}, \dots, p_{t+1}^{e_n})$ (assuming no sensing noise). We consider car control *actions* $(\alpha, \text{acc}) \in A$ composed of a steering angle $\alpha \in [0, 50]$, and discrete acceleration choice $\text{acc} \in \{\text{Accelerate}, \text{Decelerate}, \text{Maintain}\}$. The *transition probability function* $T(s_{t+1}|s_t, a_t) \in [0, 1]$ simulates the execution of action a_t in the environment state s_t for a time duration of Δt , using the bicycle kinematics model [23] to update the car states. Exo-agents are assumed to move to their goal in a straight line. The *reward function* R is defined so to reward reaching the ego-car's goal as quickly as possible while heavily penalizing collisions and near misses. The *discount factor* $\gamma = 0.98$ favors near over future rewards. For more details, we refer to [1], [17].

III. HYBRID SOLUTION HYPLAN

A. Overview

HyPlan is a learning-assisted online POMDP planner that solves the above mentioned collision-free navigation problem. For this purpose, it integrates exo-agent trajectory

¹CARLA: carla.org

²HyPlan, CARLA-CTS2, baselines: git.opendfki.de/donald.pfaffmann/HyPlan

¹Saarland University, Computer Science Dept., Saarbrücken, Germany.

²German Research Center for Artificial Intelligence (DFKI), Saarbrücken, Germany. Contact: matthias.klusch@dfki.de

³French National Centre for Scientific Research (CNRS), LAAS-CNRS, Toulouse, France. Contact: marcel.steinmetz@cnrs.fr

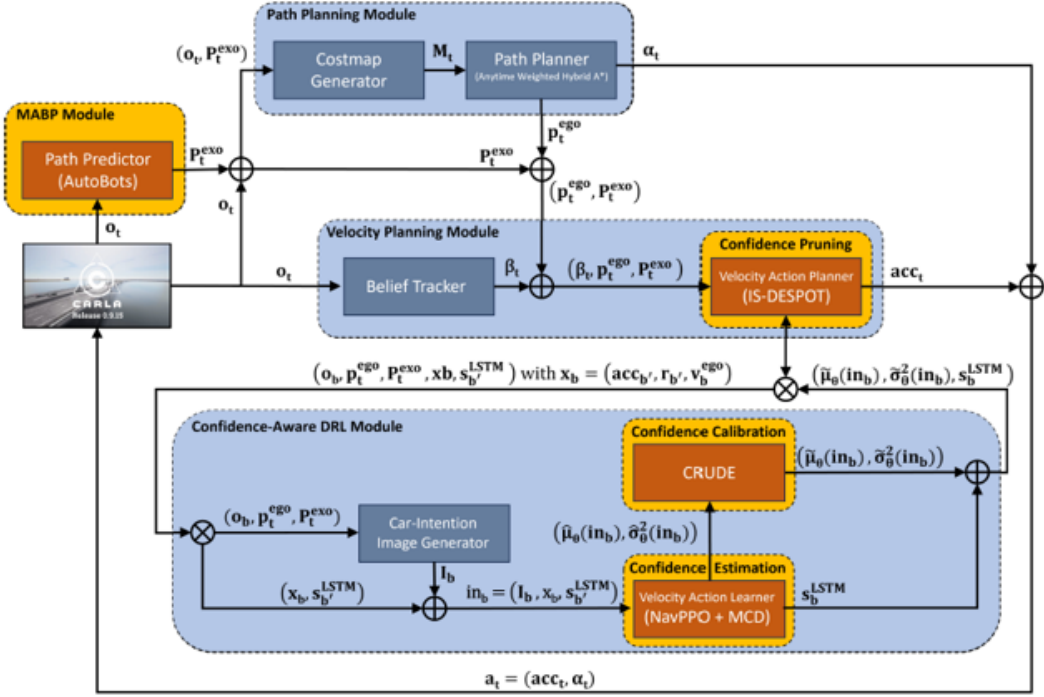


Fig. 1. Overview of HyPlan architecture with CARLA

prediction, ego-car path planning, deep reinforcement learning with proximal policy optimization, and explicit online POMDP planning with heuristic DRL confidence-based vertical pruning to obtain an approximately optimal control action policy for the ego-car (cf. Fig. 1, Alg. 1).

```

Input      : Initial belief  $b_0$ 
Output     : Control action pair  $(\alpha, acc)$ 
Parameters : Multi-agent behavior predictor MABP,
               Velocity planner VelocityPlanner
 $c \leftarrow$  car state in  $b_0$ ;
 $e_1^o, \dots, e_n^o \leftarrow$  observable states of exo-agents in  $b_0$ ;
 $P^{e_1}, \dots, P^{e_n} \leftarrow$  MABP  $(e_1^o, \dots, e_n^o)$ ;
 $P^c \leftarrow$  PathPlanner();
 $\alpha \leftarrow$  steering angle given  $c$  and  $P^c$ ;
 $acc \leftarrow$  VelocityPlanner();
return  $(\alpha, acc)$ ;
module PathPlanner():
   $M \leftarrow$  generate costmap representing  $c, P^{e_1}, \dots, P^{e_n}$ ;
   $p^c \leftarrow$  HybridAstar( $c, M$ );
  return  $p^c$ ;

```

Algorithm 1: High-level HyPlan algorithm

In short, HyPlan separates planning for the steering from velocity control of the ego-car, which polls the next control actions with a frequency of 4 Hz. More concretely, in each call, the predictor AutoBots [14] passes exo-agent trajectory predictions to the anytime weighted hybrid A* path planner [11]. This ego-car path planner generates the respectively enriched costmap upon which it computes the shortest safe path to the goal position in the actual traffic scene. The next steering action for the ego-car is derived from this planned path, while the corresponding best acceleration action for

ego-car velocity is determined by the online POMDP planner IS-DESPOT*. This hybrid planner IS-DESPOT* extends the prominent approximated online POMDP action planner IS-DESPOT [25] with belief state evaluation by the PPO-based deep reinforcement learner NavPPO. During deployment, HyPlan uses confidence calibration to correct small inconsistencies in the NavPPO belief state estimates, while its planner IS-DESPOT* leverages confidence-based vertical pruning to reduce the planning effort without impact on the planning result. During the training phase, the NavPPO network learns to behave as an experience-based critic of the IS-DESPOT* planner during its planning. As confidence calibration requires an already trained network, the training (cf. Alg. 2, Sect. III-B) and deployment (cf. Alg. 4, Sect. III-C) of HyPlan slightly differ.

B. Training of HyPlan

The training modules and procedure of HyPlan are described in Alg. 2 and Alg. 3. During training, the velocity planning module of HyPlan utilizes the hybrid POMDP planner IS-DESPOT* to compute the velocity action of the ego-car. The planner requires heuristic functions L and U that lower, respectively, upper bound the expected cumulative reward of the belief nodes created during the belief tree construction for each time step of considered training scene. It terminates a planning trial in the belief tree at some belief node b , if the bound gap $E(b) = L(b) - U(b)$ between the heuristic lower and upper bound of its state evaluation is sufficiently small. For the lower-bound heuristic during training, we fall back to a simple function $L_{tr}(b)$ that returns the collision penalty discounted by the number of steps until an exo-agent and ego-car moving towards each other collide first.

The heuristic upper bound $U(b)$ is determined by the deep reinforcement learner NavPPO. In fact, during the training phase of HyPlan, its NavPPO network learns to best estimate the values of given belief states as a heuristic upper bound for IS-DESPOT.

```

Parameters : NavPPO critic  $V_\theta$ ,
              Lower bound  $L_{tr}$ 
module VelocityPlanner () :
  def  $L(b_t)$ :
    return  $L_{tr}(b_t)$ ;
  def  $U(b_t)$ :
    return NavPPO ( $b_t$ );
   $\pi^{\text{IS-DESPOT}^*} \leftarrow \text{IS-DESPOT}^*(b_0)$  using  $L$  and  $U$ ;
  return sample acc from  $\pi^{\text{IS-DESPOT}^*}$ ;
module NavPPO ( $b_t$ ) :
   $I_{b_t} \leftarrow$  generate intention image for  $b_t$  and
   $P^c, P^{e_1}, \dots, P^{e_n}$ ;
  return  $V_\theta(I_{b_t})$ ;

```

Algorithm 2: HyPlan modules during training

The NavPPO network (cf. Fig. 2) follows a classic actor-critic approach, in which both the policy and the value function are modeled via two separate output heads, but share a common visual feature encoder. The input to NavPPO is (a) an RGB car intention image $I \in \mathbb{R}^{84 \times 84 \times 3}$ that enriches the ego-car path planner's costmap with the predicted exo-agent paths, the past and the planned path of the car in the scene, and (b) non-visual state features $\mathbf{x}_t^{\text{in}} = (r_{t-1}, acc_{t-1}, v_t^c)$, which are the previously obtained reward, the last executed velocity action and the current velocity of the ego-car. The visual processing of the car intention image is done by a sequence of three-layered convolutional neural networks and normalization followed by fully connected layer for final flattening into a latent feature map representation vector that is concatenated with the state vector $\mathbf{x}_t^{\text{in}} \in \mathbb{R}^5$ to serve together with the LSTM state s_{t-1}^{LSTM} from the previous scene step the final determination of the stochastic action policy $\pi_\psi(\cdot \mid I_t, s_{t-1}^{\text{LSTM}}, x_t^{\text{in}}) \in \mathbb{R}^3$ (actor) and the state value estimate $V_\theta(I_t, s_{t-1}^{\text{LSTM}}, x_t^{\text{in}}) \in \mathbb{R}$ (critic, in short: $V_\theta(b)$). In particular, the updated hidden state h_t of the new LSTM state $s_t^{\text{LSTM}} = (h_t, c_t)$ branches into two independently trained output paths: The upper path realizes the policy function (*Actor*) by means of a fully connected layer that maps the 128-dimensional LSTM output onto three neurons, representing the logits of a distribution over all possible velocity actions and thus defining the stochastic policy π_ψ , while the lower path approximates the value function by means of a fully connected layer that maps the LSTM output onto a single neuronal unit that provides the scalar value estimate $V_\theta(b)$. An upstream MC dropout layer is only active during deployment (cf. Section III-C).

NavPPO uses a PPO-based loss function $J(\theta, \psi)$ for its on-policy learning of constrained imitation of the planner policy based on the relative quotient of both policies $\pi_\psi(acc_t \mid \cdot)$ and $\pi_t^{\text{IS-DESPOT}^*}(acc_t \mid \cdot)$ weighed with the estimated benefit of the planned action:

$$J(\theta, \psi) = -J_\pi(\psi) + c J_V(\theta) + \lambda_{\text{reg}} (\|\theta\|_2^2 + \|\psi\|_2^2), \text{ with}$$

```

Input :  $N$  scenes for training
         $M$  scenes for calibration
        Number of stochastic forward passes  $F$ 
        HyPlan PPO loss function  $J_{\text{HyPlan}}$ 
        Max simulation time steps  $T_{\text{max}}$ 
Output : NavPPO critic  $V_\theta$ , and
          CRUDE calibration parameters  $\zeta$ 
Initialize actor and critic parameters  $\psi$  and  $\theta$ ;
foreach training scene do
   $B \leftarrow \emptyset$ ;
   $b_0 \leftarrow$  initial belief of the scene;
  foreach time step  $t = 0, \dots, T_{\text{max}} - 1$  do
     $a_t \leftarrow \text{HyPlan}(b_t)$ ;
     $\pi_t^{\text{IS-DESPOT}^*} \leftarrow$  the corresponding IS-DESPOT $^*$ 
    policy;
     $o_t, r_t \leftarrow$  execute  $a_t$  in the scene;
     $b_{t+1} \leftarrow$  update belief according to  $o_t$ ;
    add  $(b_t, \pi_t^{\text{IS-DESPOT}^*}, r_t, b_{t+1})$  to  $B$ ;
  end
  Update  $\theta$  and  $\psi$  so to minimize  $J_{\text{HyPlan}}(\theta, \psi)$  over  $B$ 
  via stochastic gradient descent;
end
 $E \leftarrow \emptyset$ ;
foreach calibration scene do
   $B \leftarrow \emptyset$ ;
   $b_0 \leftarrow$  initial belief of the scene;
  foreach time step  $t = 0, \dots, T_{\text{max}} - 1$  do
     $a_t \leftarrow \text{HyPlan}(b_t)$ ;
     $o_t, r_t \leftarrow$  execute  $a_t$  in the scene;
     $b_{t+1} \leftarrow$  update belief according to  $o_t$ ;
     $\mu_t, \sigma_t^2 \leftarrow$  statistics of  $F$  calls to NavPPO ( $b_t$ )
    with different dropout masks;
    add  $(\mu_t, \sigma_t^2, r_t)$  to  $B$ ;
  end
   $E \leftarrow E \cup \{(\hat{A}_t - \mu_t)/\sigma_t \mid 0 \leq t < T_{\text{max}}$ ,
  advantage score  $\hat{A}_t$  in  $B$  at time  $t\}$ ;
end
 $\zeta \leftarrow$  fit empirical error distribution to  $E$ ;
return  $(V_\theta, \zeta)$ ;

```

Algorithm 3: HyPlan training procedure

$$J_\pi(\psi) = \mathbb{E}_{t \sim \tau} \left[\min \left(\rho_t(\psi) \hat{A}_t, C(\rho_t(\psi), 1 - \epsilon, 1 + \epsilon) \hat{A}_t \right) \right]$$

$$\rho_t(\psi) = \frac{\pi_\psi(acc_t \mid I_t, s_{t-1}^{\text{LSTM}}, x_t^{\text{in}})}{\pi_t^{\text{IS-DESPOT}^*}(acc_t \mid b_t)}, \text{ and } J_V(\theta) = \mathbb{E}_{t \sim \tau} [\hat{A}_t^2]$$

where θ (critic) and ψ (actor) are the network weights to be trained and updated periodically after each episode, and \hat{A}_t denotes the generalized advantage estimate (GAE) at time step t

$$\hat{A}_t = \sum_{l=0}^{T-t-1} (\gamma \lambda)^l \delta_{t+l}, \text{ with temporal-difference residual}$$

$$\delta_t = r_t + \gamma V_\theta(I_{t+1}, s_t^{\text{LSTM}}, x_{t+1}^{\text{in}}) - V_\theta(I_t, s_{t-1}^{\text{LSTM}}, x_t^{\text{in}})$$

where $\lambda \in [0, 1]$ is a decay factor. The function $\rho_t(\psi)$ denotes the probability ratio between the current DRL policy π_ψ and the policy $\pi_t^{\text{IS-DESPOT}^*}(acc_t \mid b_t)$ proposed by the planner for executing action acc_t at scene simulation step t under belief b_t . $C(\cdot)$ is the clip operator that restricts $\rho_t(\psi)$ to the interval $[1 - \epsilon, 1 + \epsilon]$ to prevent excessively large policy updates, $\epsilon \in \mathbb{R}_{>0}$ the clipping threshold, $c \in \mathbb{R}_{\geq 0}$

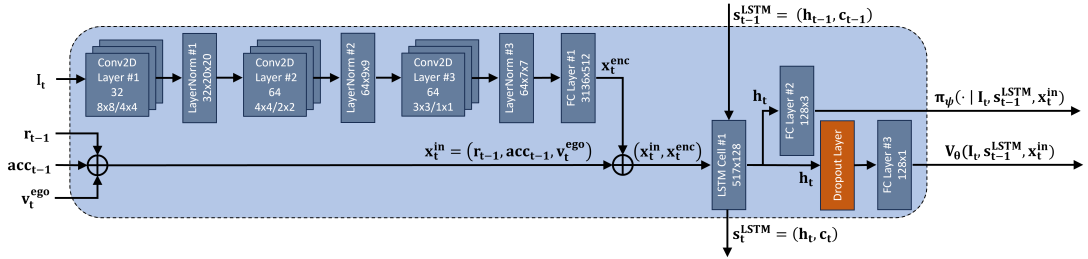


Fig. 2. DRL NavPPO network architecture

the weighting factor controlling the contribution of the value loss, and $\lambda_{\text{reg}} \in \mathbb{R}_{\geq 0}$ the regularization coefficient jointly applied to all actor-critic network parameters to prevent overfitting.

After NavPPO has been successfully trained, the NavPPO value predictions are validated over a separate calibration instance set. To this end, HyPlan is simulated over the calibration scenes, collecting during this process the mean and standard deviations of F stochastic forward passes of the NavPPO value network with Monte Carlo dropouts for each simulation step; in our experiments, we set $F = 10$. Based on the collected statistics, normed empirical errors with respect to the GAE are computed. At the end, an empirical distribution for the collected normalized errors is constructed, which during the deployment of HyPlan, serves as input to CRUDE [32] to calibrate the NavPPO value estimates and the confidence in them.

C. Deployment Architecture of HyPlan

Parameters: NavPPO critic V_θ ,
 Manually designed lower bound L_{tr} ,
 CRUDE calibration parameters ζ ,
 Number of stochastic forward passes F

```
module VelocityPlanner():
    def L(b_t):
        |  $\tilde{\mu}, \tilde{\sigma}^2 \leftarrow \text{calNavPPO}(b_t);$ 
        |  $\varphi = \text{getConfidence}(\tilde{\sigma}^2);$ 
        |  $\text{return } (1 - \varphi)L_{\text{tr}}(b_t) + \varphi\tilde{\mu};$ 
    def U(b_t):
        |  $\tilde{\mu}, \tilde{\sigma}^2 \leftarrow \text{calNavPPO}(b_t);$ 
        |  $\text{return } \tilde{\mu};$ 
     $\pi^{\text{DESPOT}} \leftarrow \text{IS-DESPOT}^*(b_0)$  using  $L$  and  $U$ ;
     $\text{return sample acc from } \pi^{\text{DESPOT}};$ 
module calNavPPO(b_t):
     $I_{b_t} \leftarrow \text{generate intention image for } b_t \text{ and}$ 
     $P^c, P^{e_1}, \dots, P^{e_n};$ 
     $\mu, \sigma^2 \leftarrow F \text{ samples of } V_\theta(I_{b_t}) \text{ using dropout};$ 
     $\tilde{\mu}, \tilde{\sigma}^2 \leftarrow \text{calibrate}(\mu, \sigma^2; \zeta);$ 
     $\text{return } \tilde{\mu}, \tilde{\sigma}^2;$ 
```

Algorithm 4: HyPlan modules during deployment

In the deployment phase of HyPlan, the online POMDP planner IS-DESPOT* additionally performs vertical pruning of its action planning based on the confidence the trained learner NavPPO has in its experience-based evaluation of belief states. More concretely, NavPPO runs multiple stochastic

forward passes with different dropout masks to obtain the mean μ of generated belief state value estimates $V_\theta(b)$ together with their variance σ^2 . The planner receives from the learner the calibrated mean $\tilde{\mu}$ of state values as heuristic upper bound $U(b)$ and the calibrated variance $\tilde{\sigma}^2$, and uses the inverse of the latter as the confidence value $\varphi \in [0, 1]$ of the learner in its evaluation of belief state b . The calibrations are performed with the standard method CRUDE [32], in particular to reduce cases of false positives³.

For each belief node b created during planning, both its state value estimation and the confidence in it by the learner are used by the planner to determine whether it is worthwhile to continue planning from b in the belief tree, or rather not. For this purpose, the planner uses the heuristic lower bound $L(b)$, which is defined as confidence-weighted sum $L(b) = (1 - \varphi_b)L_{\text{tr}}(b) + \varphi_bU(b)$ of the pre-defined heuristic lower bound $L_{\text{tr}}(b)$ as utilized during training (cf. Sect. III-B) and the heuristic upper bound $U(b)$ from the trained learner. Therefore, highly confident upper bound value estimations for selected belief states result in smaller bound gaps than those with lower confidence.

In particular, belief states with maximal upper bound value estimate and high confidence value by the learner lead to an earlier termination of the planning trial and final action selection at the root node than without this kind of vertical pruning. That heuristically avoids over-exploration of familiar regions of the belief state space by the planner for which the state value estimations returned by the learner are unlikely to change, which is indicated by the degree of confidence the learner has in them.

As a simple example of vertical pruning, consider some traffic scene simulation step for which enriched observation IS-DESPOT* starts its planning of an approximately optimal velocity action for the ego-car. Let us further assume that no collision threat would be left if accelerates at this step, such that the car could even continue accelerating until the goal is reached without any collision and NavPPO learned to recognize and evaluate such situations with high confidence. In this example, the planner reaches already on the first planning layer a belief state for simulated action "Accelerate" from the root which gets evaluated with the maximal upper

³For example, in such cases, NavPPO would return a high-confidence high-value estimate for a belief node which plan branch after node selection would later on lead to a collision, even if the car were to continuously decelerate in this branch.

bound value estimate and with high confidence by NavPPO. As a consequence, the planner terminates the whole planning trial, selects this action after the backup process to the root as heuristically optimal for this scene step, and executes it. In particular, the final selection of this action would not have changed in subsequent planning steps in this trial that would be needed without pruning. One question is whether and to what extent the potential speed-up of online POMDP planning through this learner confidence-based vertical pruning would come at the cost of safety of driving compared to other baseline methods in general.

IV. EVALUATION

We conducted an experimental comparative performance evaluation of HyPlan with selected baselines regarding safety, efficiency and planning efforts on the synthetic CARLA-CTS2 benchmark of critical traffic scenarios.

A. Experimental setting

Benchmark. The CARLA-CTS2 benchmark consists of nine parameterized scenarios with about twenty-three thousand traffic scenes with pedestrian crossing simulated with the CARLA driving simulator. These traffic scenarios are identified in the real-world in-depth accident study in Germany (GIDAS) [2] as most critical, where the car is confronted with a street crossing pedestrian, possibly occluded by some parking car, an incoming car, and different street intersections. The scenes per scenario are generated with varying speed and crossing distance of pedestrians from the car.

Baselines. The selected baseline methods for CFN problem solving are (a) the deep reinforcement learners NavPPO and NavA2C, (b) the explicit navigation planner IS-DESPOTp [25], (c) the hybrid learning-assisted planners HyLEAP [27] and LEADER [9], and (d) the hybrid planning-assisted deep reinforcement learner HyLEAR [17]. Training, calibration and testing on the benchmark followed a 25:25:50% ratio of respective sets. The explicit navigation planner IS-DESPOTp utilizes the IS-DESPOT planner [25] to obtain the approximately optimal velocity for actual steering action derived from ego-car path planned with standard hybrid A* used in all baselines.

Measurements. The performance of each method is measured in terms of (a) the overall safety index (SI90) defined as total number of scenarios in which the method fails (crash or near-miss) in 10 percentages of the scenes; (b) the crash and near-miss rates (%), and time to goal (TTG) in seconds; and (c) the execution time in milliseconds and, if applicable, training time in days. In addition, for explicit planning and hybrid methods, the effort of planning is measured in terms of average (a) planning time (PT), (b) number of planning trials (PTN), (c) planning trial depth (PTD), (d) number of belief nodes in BT (BNN), (e) observation branching factor (OBF), and (f) neural network evaluation time (NNET). HyPlan is implemented in Python and PyTorch framework; all experiments were run on the NVIDIA DGX-2 servers.

B. Results

The overall results of our experiments with respect to safety, efficiency, and, where applicable, the planning efforts of the considered methods, averaged across all scenarios, are shown in Tables I and II. For each measure, we first average the scores across all scenes of a scenario and then average across all scenarios such that each scenario is weighted equally. In general, HyPlan provided a safer ride than all baselines (cf. Table I). Moreover, its execution is significantly faster (up to 40 percent) than all other explicit and hybrid planning baselines, but still remains three to four times slower than the considered learning baselines and at the expense of the highest TTG value due to a more cautious driving behavior. The deep reinforcement learner NavPPO is fastest in training, execution and with best TTG value, but that comes at the very cost of safety. Overall, navigation with the considered hybrid methods turned out to be safer than with the tested methods of explicit planning and mere deep learning.

Regarding the planning efforts (cf. Table II), HyPlan turned out to incorporate the fastest approximate online POMDP planner (IS-DESPOT with learner confidence-based vertical pruning), with shortest planning trial depths and less belief nodes to evaluate in less planning trials on average, compared to all alternative planners. The hybrid learning-assisted planner LEADER was slowest in planning and execution but fastest in its used neural network evaluation of the situation as input to but not during planning in IS-DESPOT.

In addition, we conducted an extensive ablative study of HyPlan to investigate the impact of its individual functional components for path prediction, DRL, confidence calibration and vertical pruning in the planning process on the overall performance of the system. Among others, the results showed that compared to the full HyPlan, the best navigation safety can be achieved with its variant that avoids vertical pruning while calibrating its belief node evaluations for the planner, though at the cost of longest execution time out of all variants. On the other hand, avoiding confidence calibration resulted in over-optimistic (confidence for) vertical pruning of the planner, which led to the fastest execution time of all variants but at the cost of worst navigation safety. Interestingly, vertical pruning alone caused the respective variant of HyPlan to be significantly faster than all its other variants with planning but showed slightly less safe driving behavior than the variants without vertical pruning. The additional integration of pedestrian path prediction (and its use for planning) led to marginally increased navigation safety and reduced planning efforts but at the cost of slightly increased execution time. Finally, the combination of all new or improved methods in HyPlan compared to its variants led to the best tradeoff with respect to safety of driving and execution time.

V. RELATED WORK

As mentioned above, there exists a wide range of methods to address the problem of collision-free navigation under uncertainty. Deep learning-based approaches have become omnipresent in autonomous driving research [15], [22].

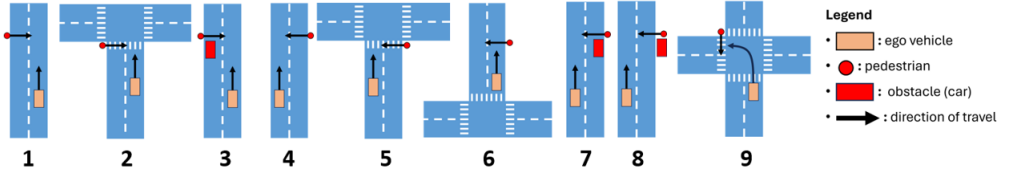


Fig. 3. Scenarios of CARLA-CTS2 benchmark with pedestrian crossing

Method	Safety	Crash (%)	Near-Miss (%)	TTG (s)	Execution (ms)	Training (d)
IS-DESPOTP	1	18.43	18.94	16.91	251.29	N/A
NavA2C	1	13.50	24.02	13.74	104.95	2.51
NavPPO	2	14.64	10.24	12.74	32.59	1.91
HyLEAR	3	13.76	14.15	15.21	41.38	3.21
HyLEAP	4	13.29	13.39	16.46	225.76	4.76
LEADER	4	12.64	16.67	16.72	267.43	5.01
HyPlan	7	12.36	8.04	19.97	161.17	4.33

TABLE I

EXPERIMENTAL RESULTS FOR NAVIGATION SAFETY AND EFFICIENCY OF HYPLAN AND BASELINES OVER BENCHMARK CARLA-CTS2

Method	PT (ms)	NNET (ms)	BNN	PTN	PTD	OBF
IS-DESPOTP	244.72	N/A	543	43.91	9.29	1.23
HyLEAP	218.71	187.93	39.54	2.36	6.46	1.15
LEADER	259.58	6.76	568	45.73	9.47	1.32
HyPlan	149.94	116.52	15.62	3.62	2.21	0.93

TABLE II

EXPERIMENTAL RESULTS FOR PLANNING EFFORTS OF EXPLICIT AND HYBRID PLANNERS OVER CARLA-CTS2.

PT: PLANNING TIME; BNN: #BELIEF NODES; PTN: #PLANNING TRIALS; PTD: PLANNING TRIAL DEPTH; OBF: OBSERVATION BRANCHING FACTOR; NNET: NEURAL NETWORK EVALUATION TIME.

These approaches span from learning vehicle control policies [21], e.g., via deep reinforcement learning, operating on semantic environment features, to end-to-end learning approaches [7], such as UniAD [16], that consolidate the entire autonomous driving decision pipeline into a single deep neural network. Sparked by the success of LLMs in other decision-making tasks, the use of LLMs for autonomous driving is receiving significant attention lately such as [6], [10], [19], [29]–[31] with noticeable success on relevant benchmarks such as nuPlan [26]. For example, LMdrive [29] leverages a multi-modal LLM, which fuses language instructions with camera and LiDAR sensor data to low-level control outputs. However, since the decision-making process is entirely based on black-box models, these end-to-end learning approaches suffer from severe predictability and robustness issues [7]. By combining experience-based with explicit planning approaches, those issues are much less pertinent in HyPlan. In general, the use of LLMs as planners without any integrated logic-based verification as safeguard [24] does not yield logically provable correct planned policies with guarantees [5].

Alternative neuro-explicit planning approaches are by no means new and have been explored in various works in the past [3], [9], [27], [28]. At a high level, one can classify these hybrid approaches into learning-assisted planners and planning-assisted learners. As an example for planning-assisted learners, HyLEAR [17] uses an explicit planner

to improve training of a vehicle behavior-control policy that optimizes simultaneously the satisfaction of passenger preferences and traffic rules as well as avoiding collisions. More relevant to HyPlan is the category of learning-assisted explicit planners. For instance, LEADER [9] learns a model predicting pedestrian intentions, which is used to steer the Monte Carlo sampling in their explicit IS-DESPOT planner to critical situations. This is orthogonal to HyPlan, which leverages an external behavior predictor to construct more informed inputs for an explicit path planner and the PPO-based belief node estimator. LFG [28] uses common knowledge embedded into LLMs in order to implement a search guidance heuristic for a navigation planner that takes a natural language goal. Similarly, HyPlan leverages an experience-based search guidance heuristic. However, the heuristic in HyPlan is not designed to support natural language goals and is optimized directly for the purpose of guiding its explicit POMDP planner IS-DESPOT through the learner NavPPO imitating the planner policy.

VI. CONCLUSION

We presented HyPlan, a novel hybrid learning-assisted online POMDP planner for collision-free driving control action policies for autonomous cars. The experimental results over the CARLA-CTS benchmark revealed that HyPlan can outperform all selected baselines in terms of safety. Moreover, it is significantly faster than all selected explicit planning-

based methods in training and execution time, and further reduces but does not yet close the existing inference speed gap to the mere deep learning-based CFN methods.

REFERENCES

- [1] Bai, H., Cai, S., et al. (2015). Intention-aware online POMDP planning for autonomous driving in a crowd. Proc. International Conference on Robotics and Automation (ICRA). IEEE.
- [2] Bartels, B. & Liers, H. (2014): Bewegungsverhalten von Fußgäengern im Straßenverkehr, Teil 2. FAT-Schriftenreihe, Nr. 268.
- [3] Cai, P., & Hsu, D. (2022). Closing the planning–learning loop with application to autonomous driving. *IEEE Transactions on Robotics*, 39(2). IEEE.
- [4] Cannizzaro, R., & Kunze, L. (2023). Car-DESPOT: Causally-informed online pomdp planning for robots in confounded environments. Proc. IEEE/RSJ International Conference on Intelligent Robots and Systems (IROS). IEEE.
- [5] Cao, P., Men, T., et al. (2025). Large language models for planning: A comprehensive and systematic survey. arXiv preprint arXiv:2505.19683.
- [6] Chen, Y., Ding, Z.H., et al. (2024). Asynchronous large language model enhanced planner for autonomous driving. Proc. European Conference on Computer Vision (ECCV). Springer.
- [7] Chen, L., Wu, P., et al. (2024). End-to-end autonomous driving: Challenges and frontiers. *IEEE Transactions on Pattern Analysis and Machine Intelligence*, 46(12). IEEE.
- [8] Cui, C., et al. (2024). A survey on multimodal large language models for autonomous driving. Proc. IEEE/CVF Winter Conference on Applications of Computer Vision.
- [9] Danesh, M.H., Cai, P., & Hsu, D. (2023). LEADER: Learning attention over driving behaviors for planning under uncertainty. Proc. International Conference on Robot Learning (CoRL). PMLR.
- [10] Dauner, D., et al. (2023). Parting with misconceptions about learning-based vehicle motion planning. Proc. of Machine Learning Research (PMLR) for Conference on Robot Learning (CoRL). See also: Dauner, D., et al. (2023). Predictive Driver Model: A Technical Report.
- [11] Dolgov, D., Thrun, S., Montemerlo, M., & Diebel, J. (2010). Path planning for autonomous vehicles in unknown semi-structured environments. *Robotics Research*, 29(5).
- [12] Everett, M., Chen, Y.F., & How, J.P. (2021): Collision avoidance in pedestrian-rich environments with deep reinforcement learning. *IEEE Access*, 9:10357–10377. IEEE.
- [13] Gariboldi, C., Tokida, H., Kinjo, K., Asada, Y., & Carballo, A. (2025). VLAD: A VLM-Augmented Autonomous Driving Framework with Hierarchical Planning and Interpretable Decision Process. arXiv preprint arXiv:2507.01284.
- [14] Girgis, R., et al. (2021). Latent variable sequential set transformers for joint multi-agent motion prediction. arXiv preprint arXiv:2104.00563.
- [15] Grigorescu, S., Trasnea, B., Cocias, T., & Macesanu, G. (2020). A survey of deep learning techniques for autonomous driving. *Field Robotics*, 37(3).
- [16] Guo, M., Zhang, Z., He, Y., Wang, K., & Jing, L. (2024). End-to-end autonomous driving without costly modularization and 3d manual annotation. arXiv preprint arXiv:2406.17680.
- [17] Gupta, D. & Klusch, M. (2023): Hybrid deep reinforcement learning and planning for safe and comfortable automated driving. Proc. 34th IEEE International Intelligent Vehicles Symposium (IV), IEEE.
- [18] Hu, Y., et al. (2023). Planning-oriented autonomous driving. Proceedings of the IEEE Conference on Computer Vision and Pattern Recognition (CVPR). IEEE.
- [19] Hwang, J. J., Xu, R., et al. (2024). Emma: End-to-end multimodal model for autonomous driving. arXiv preprint arXiv:2410.23262.
- [20] Jiang, B., Chen, S., Xu, Q., Liao, B., Chen, J., Zhou, H., ... & Wang, X. (2023). VAD: Vectorized scene representation for efficient autonomous driving. Proc. IEEE/CVF International Conference on Computer Vision.
- [21] Kendall, A., Hawke, J., et al. (2019). Learning to drive in a day. Proc. IEEE International Conference on Robotics and Automation (ICRA). IEEE.
- [22] Kiran, B.R., et al. (2021). Deep reinforcement learning for autonomous driving: A survey. *IEEE Transactions on Intelligent Transportation Systems*, 23(6). IEEE.
- [23] Kong, J., Pfeiffer, M., Schildbach, G., & Borrelli, F. (2015). Kinematic and dynamic vehicle models for autonomous driving control design. Proc. IEEE Intelligent Vehicles Symposium. IEEE.
- [24] Lee, C.P., Porfirio, D., et al. (2025). Veriplan: Integrating formal verification and ILMs into end-user planning. Proc. CHI Conference on Human Factors in Computing Systems.
- [25] Luo, Y., et al. (2019): Importance sampling for online planning under uncertainty. *Robotics Research*, 38(2-3).
- [26] nuPlan Benchmark for autonomous vehicle planning. <https://www.nuscenes.org/nuplan>
- [27] Pusse, F., & Klusch, M. (2019): Hybrid online POMDP planning and deep reinforcement learning for safer self-driving cars. Proc. IEEE Intelligent Vehicles Symposium (IV). IEEE.
- [28] Shah, D. et al. (2023). Navigation with large language models: Semantic guesswork as a heuristic for planning. Proc. of Machine Learning Research (PMLR) for Conference on Robot Learning.
- [29] Shao, H., Hu, Y., et al. (2024). Lmdrive: Closed-loop end-to-end driving with large language models. Proc. IEEE/CVF Conference on Computer Vision and Pattern Recognition.
- [30] Sharan, S.P., Pittaluga, F., & Chandraker, M. (2023). Llm-assist: Enhancing closed-loop planning with language-based reasoning. arXiv preprint arXiv:2401.00125.
- [31] Tian, X., Gu, J., et al. (2024). Drivevlm: The convergence of autonomous driving and large vision-language models. arXiv preprint arXiv:2402.12289.
- [32] Zelikman, E., et al. (2020). CRUDE: calibrating regression uncertainty distributions empirically. arXiv preprint arXiv:2005.12496.